energies

MDPI

Article

Closed Solar House with Radiation Filtering Roof for Transplant Production in Arid Regions: Energy Consumption

Ahmed M. Abdel-Ghany [1,*], Ibrahim M. Al-Helal [1], Abdullah A. Alsadon [2], Abdullah A. Ibrahim [2] and Mohamed R. Shady [1]

[1] Department of Agricultural Engineering, College of Food and Agriculture Sciences, King Saud University, P.O. Box 2460, Riyadh 11451, Saudi Arabia; imhelal@ksu.edu.sa (I.M.A.-H.); mshady@ksu.edu.sa (M.R.S.)

[2] Department of Plant Production, College of Food and Agriculture Sciences, King Saud University, P.O. Box 2460, Riyadh 11451, Saudi Arabia; alsadon@ksu.edu.sa (A.A.A.); adrahim@ksu.edu.sa (A.A.I.)

* Correspondence: aghany@ksu.edu.sa; Tel.: +966-5-4137-4952; Fax: +966-1-46-78502

Academic Editor: Timothy Anderson

Received: 14 November 2015; Accepted: 16 February 2016; Published: 26 February 2016

Abstract: Under harsh weather conditions, closed transplant production systems (CTPS) are currently used to produce high quality transplants under artificial lighting. More than 70% of the electric energy consumed in the CTPS is for lighting. This article presents a simulation study to examine the possibility of using an alternative closed solar house, with radiation filtering roof, for transplant production in hot sunny regions to replace the artificial lighting in the CTPS with sunlight. The sidewalls of the house were insulated as in the CTPS and the roof was transparent, and made from polycarbonate hollow-channeled structure. There was a liquid radiation filter (LRF) (1.5% $CuSO_4$–water solution) flowing in a closed loop through the roof channels to absorb the solar heat load (*i.e.*, the near infra-red radiation, NIR: 700–2500 nm) and transmit the photosynthetically active radiation (PAR: 400–700 nm) for plant growth. The LRF inlet temperature was assumed to be 25 °C to prevent vapor condensation on the inner surface of the cover. The evapo-transpired water vapor was removed immediately to maintain the relative humidity inside the house at 70%. The results proved that this technique can offer an appropriate air temperature inside the house less than outside air temperature by around 8–10 °C in hot summer days, and the integrated electric energy consumption during the production period was estimated to be around 43% of the CTPS consumption.

Keywords: fluid-roof; hot desert; solar radiation; transplants production; radiation filter

1. Introduction

Farmers in arid regions (hot and sunny deserts), such as in the Arabian Peninsula, are producing vegetable transplants either in open fields or in the greenhouses; *i.e.* the open transplant production systems (OTPS). In hot summer seasons, cooling the greenhouses is necessary to provide a suitable environment for transplant growth. The cooling systems (*i.e.*, evaporative cooling) often used in these areas face many operational difficulties due to the high salinity of water resources. On the other hand, transplant production in open fields faces many problems, especially in summer, due to the high radiation intensity along with high wind speed as well as high air temperature, resulting in a high percent of wilting of transplant during production. Wilting of transplants delays the growing season and affects the final production and, consequently, the market prices of vegetables increase. Therefore, OTPS for transplant production in hot regions is not economically profitable. Promising technology has been developed in Japan, which has succeeded and been commercialized in large

scales [1], later transferred to South Korea and China [2], for producing transplants in closed systems, called "closed transplant production systems" (CTPS), under artificial light using fluorescent lamps as a photosynthetic photon flux (PPF) source. CTPS is a thermally insulated and nearly airtight warehouse-like opaque structure. CTPS are able to produce high quality transplants with high photosynthetic ability using minimum resources and environmental pollution [3]. CTPS produce healthy transplants, able to produce high yields after planting in open fields or greenhouses [4,5]. There are many environmental and economical advantages for CTPS over OTPS, such as easier and faster production of pathogen-free transplants; high quality from adapting a more accurate controlled environment [6]; and more efficient space utilization by introducing multi-layer shelves in the CTPS [7,8]. Extensive previous studies revealed that the use efficiencies (*i.e.*, the amount of the resource fixed or held in plants to the amount of the resource supplied to the CTPS) of CO_2, water, and light energy are considerably higher in CTPS than those in a greenhouse [9]. Accordingly, CTPS are appropriate technique that can be applied in hot and sunny regions during summer seasons for protecting and saving transplants from the prevailing adverse environmental conditions. However, most of the electric energy consumptions in the CTPS are consumed mainly for lighting. It has been estimated to be around 75% of the total energy consumption [10]. In most cases, the requirement of electric energy to produce transplants in CTPS is much higher than the transplant production in the greenhouse because the light source in the greenhouse is free (sunlight). In hot sunny regions such as in the Middle East and in the Arabian Peninsula, an intensive solar radiation is available all year round and is more than sufficient for transplant and crop production (annual average of daily global irradiance is 22–28 $MJ \cdot m^{-2} \cdot d^{-1}$) [11,12]. Most new farms in these regions are in the desert where electricity networks are not available and water resources are brackish. Therefore, a closed solar house with a fluid-roof cover (FRC) is proposed, similar to CTPS. This is to provide a suitable internal environment for transplant growth and to use the free light source (sunlight) instead of electricity.

To reduce the solar heat load inside the buildings in hot and sunny regions, the concept of the fluid roof cover (FRC) has been used since 1893, first by Van Der Heyden (Patent No. US-504544), to design sanitary house. He used Kali-alumen [$KAL(SO_4)_2$] and Ammonia-alumen [$NH_4AL(SO_4)$] in water to make solutions to be used between a double-walled glass roof, performing FRC [13]. Such FRCs act as the commercial shading materials (e.g., plastic nets, thermal screens, curtains, *etc.*); they reduce the transmission of solar radiation across the whole solar spectrum range including the photosynthetically active radiation (PAR). However, a liquid radiation filter (LRF) selectively absorbs the ultraviolet (UV) and NIR wave bands and highly transmits the PAR by selecting solutions with suitable optical properties. Therefore, LRFs have been investigated and used in several studies for shading a greenhouse roof instead of other shading methods. Cupper chloride–water solution (3% concentration) [14–16] and the copper sulfate ($CuSO_4$)–water solution (1.5% concentration) [17,18] were used as LRFs by flowing it through double-layer, rigid plastic, greenhouse covers to reduce the inside air temperature.

Because of the significant effects of the LRF on the light quality inside greenhouses (*i.e.*, the transmission ratios of red/far-red, blue/red and blue/far-red), copper sulfate–water solutions (LRF) have been used as a method to regulate the plant morphology in photo-morphogenesis studies [19–22] and to reduce plant transpiration rate [23]. In 1991, Levi *et al.* developed a new LRF (F_e^{+++} based-water solution) [24]; this LRF was evaluated by using it for FRC in greenhouses in a hot desert [25,26]. However, the spectral radiative properties of this LRF in solar spectrum bands were not published. Up to the last decade, the FRC with a selective LRF was the unique solution to regulate the solar radiation and air temperatures in greenhouses [25,26]. To avoid complexity and the possible hazards of the LRF, such as $CuSO_4$–water solution, efforts have been made to develop transparent covering materials (rigid sheets or films) to act as LRF [27,28]. However, the deterioration of mechanical and physical properties of these products was very fast under extensive solar radiation conditions.

The present simulation study is to design a closed solar house using the advantages of CTPS for producing high quality, low-cost transplants. In the proposed house, CTPS artificial lighting is replaced

by natural sunlight. The cover of the proposed house is FRC with LRF to selectively absorb the solar heat load (UV + NIR). The sidewalls of the house are assumed to be similar to CTPS sidewalls (*i.e.*, constructed from low cost, thermally insulated, and locally available materials) to prevent heat energy from entering the house, and the roof is assumed to be hollow-channeled polycarbonate structure. A LRF (1.5% $CuSO_4$–water solution) is assumed to flow in closed loop through the roof channels for filtering out the solar radiation by absorbing the heat load (UV: 200–400 nm + NIR: 700–2500 nm) and transmitting the photosynthetically active radiation (PAR: 400–700 nm) for transplant use. The hot LRF exiting from the cover will be cooled down to 25 °C using a water cooler. This study is mainly to examine the possibility of using a closed solar house with radiation filtering roof for producing transplants in arid regions and to compare the energy consumption with that in CTPS.

2. Energy Analysis

The suggested solar house used for transplant production is illustrated, not to scale, in Figure 1a. This figure illustrates the outline dimensions of the house, and different modes of energy exchange among its components (*i.e.*, the cover, transplant trays, soil surface and inside air). Figure 1b illustrates the transplant tray used for the study. Energy exchanges among the house components are as follows.

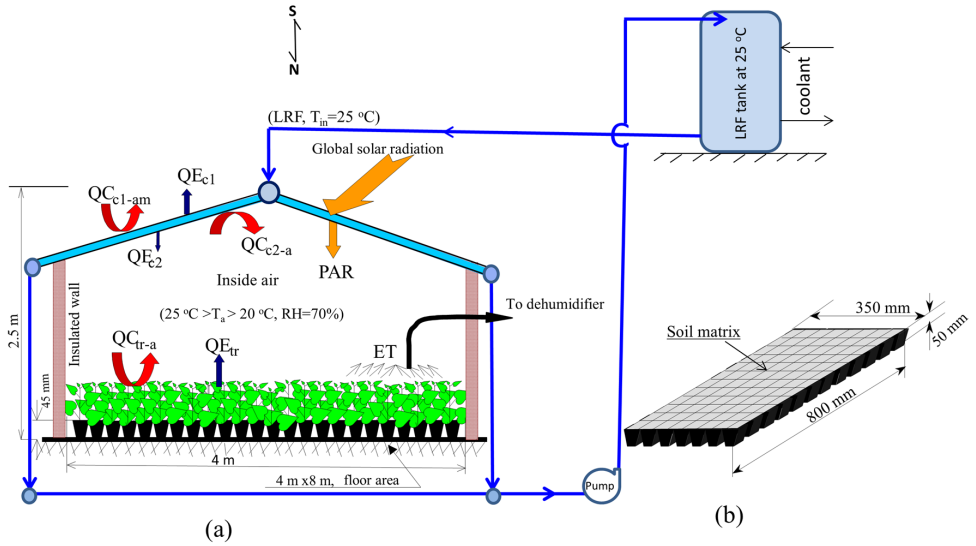

Figure 1. (**a**) Schematic diagram of the fluid-roof solar house and (**b**) view of the transplants tray used in the closed transplant production system (CTPS) and in the simulation.

2.1. The Fluid-Roof Cover (FRC)

Polycarbonate hollow-channeled fluid-roof cover (Figure 2) consists of identical rectangular channels (15 mm × 35 mm) and LRF flowing inside them. Each channel is bounded by the surfaces of two identical vertical side webs, w (d_w = 2 mm thick), and the inner surfaces of the upper and lower sheets (c_1 and c_2, d_c = 2 mm thick) (see Figure 2). A model describing the solar radiation transmitted from the cover and absorbed in the cover elements (upper sheet, c_1; lower sheet, c_2; web, w; and LRF) was established and reported in [29]. In this model, the multiple reflections of solar radiation among c1, c2 and w were considered in addition to the multiple reflections inside the elements materials as well. The input data to this model are cover dimensions and the optical constants of the LRF and cover material. The LRF (1.5% $CuSO_4$–water solution) is a clear, semi-transparent and very light blue solution; therefore, its thermo-physical properties were taken as water properties. The mass flow rate and velocity of the LRF in each channel were estimated to be 0.00525 kg·s^{-1} and 0.01 m·s^{-1}, respectively. The output parameters are the cover (FRC) transmittance and reflectance and the absorptance of the cover elements (c_1, c_2, w and LRF). The transmittances of this FRC to the

PAR and NIR were estimated to be 0.63 and 0.08, respectively [29]. This means the cover can reject 92% of the solar heating load (NIR) before entering the house. For the present simulation study, the inner surface temperature of the FRC (T_{c2}) is needed to quantify the convection heat exchange with the inside air. The cover length is divided into N divisions in the LRF flow direction (N = 20 per meter length). The temperature profile was assumed to exist in the LRF flow direction only and the temperature profile in the direction of the cover width was neglected due to the uniformity of the incident radiation over the cover and the similarity of the flow pattern in the channels. One channel was chosen (Figure 2) to study the energy balance of the FRC. A control volume (the boundary through which the energy and mass exchange with the surrounding) was chosen for each division i (i = 1, 2, ... N) (Figure 2). An energy balance was applied to each element of the division i (*i.e.*, the upper sheet ($c_{1,i}$), lower sheet ($c_{2,i}$), web (w_i) and LRF_i) in the control volume. Each element was treated as lumped heat capacity system in transient conditions with equivalent properties and an instantaneous temperature. A number of 4N differential equations describing the energy balance of each element in the division i in the 4 N unknowns $T_{c1,i}$, $T_{c2,i}$, $T_{w,i}$ and $T_{LRF,i}$, (i = 1, 2, ... N), respectively, were developed and reported in [30]. By solving these equations simultaneously, the values of $T_{c2,i}$ could be determined at any time of the day to be used in the upcoming analysis.

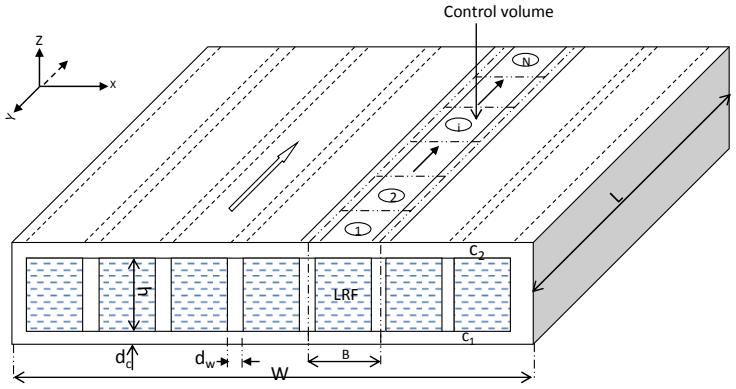

Figure 2. Schematic diagram of the hollow-channeled, fluid-roof cover, and channel dimensions (B = 35 mm, h = 15 mm, d_c = 2 mm and d_w = 2 mm).

2.2. The Inside Air

The non-absorbing non-emitting inside air is treated as one unit with average temperature T_a. The air inside the house exchanges sensible heat (convection) with the FRC, transplant trays, and floor. The sidewalls of the house were insulated as CTPS and supposed to be constructed from low cost, low thermally-conducted local materials available in desert regions. Therefore, the different modes of energy exchange between the sidewalls and the inside air were neglected. The evapo-transpired water vapor from the transplant trays is assumed to be more or less removed immediately via a dehumidifier to maintain inside relative humidity (RH) equals to 70% (the desired value for transplant growth). Energy balance of the inside air is given by:

$$QC_{c2-a} + QC_{tr-a} + QC_{f-a} + \kappa(ET - M_{dh}) = \frac{d}{dt}\left[m_T C_p T\right]_a \quad (1)$$

where QC_{c2-a}, QC_{f-a} and QC_{tr-a} are the convected heat from the inner surface of the cover, from the floor uncovered with transplant trays and from the transplant tray-substrate units to the inside air, respectively. ET is the evapo-transpiration rate from the transplant trays (Section 3.3) and M_{dh} is the mass of vapor condensed by the dehumidifier and is given by:

$$M_{dh} = m_D\left[\omega_a - 0.75\omega_{as}\frac{(1 - p_{vs}/p_t)}{(1 - 0.75p_{vs}/p_t)}\right] \quad (2)$$

where ω_a, ω_{as}, m_T and m_D are the humidity ratio of the air, the humidity ratio of the saturated air, mass of the moist air and mass of the dry air in the proposed solar house, respectively. In addition, p_{vs} and p_t are the partial pressure of water vapor of the saturated air and the total pressure, respectively, inside the house. The convected heat from the inner surface of the cover to the inside air, QC_{c2-a}, depends on the cover element temperature, $T_{c2,i}$ (i = 1, 2, 3, ... N) and the inside air temperature, T_a. Thus, QC_{c2-a} is given by:

$$QC_{c2-a} = N_c \sum_{i=1}^{N} A_i h_{c2,i-a}(T_{c2,i} - T_a) \quad (3)$$

where A_i and $h_{c2,i-a}$ are the surface area of the cover element i and the convection heat transfer coefficient between the element i and the inside air, respectively. A natural convection mechanism exists on the different surfaces inside the closed house (*i.e.*, the inner surface of cover, transplant leaves, soil substrate and floor lanes uncovered with trays). Thus, $h_{c2,i-a}$ is given by [31] as:

$$\begin{array}{ll} h_{c2,i-a} = Nu.k_a/L, & \\ Nu = 0.76Ra^{1/4} & 10^4 < Ra < 10^7 \\ Nu = 0.15Ra^{1/3} & 10^7 < Ra < 3 \times 10^{10} \end{array} \quad (4)$$

where Ra, Nu, k_a and L are Rayleigh number, Nusselt number, thermal conductivity of air and the characteristic length of the element, i (4 × area/perimeter), respectively.

The convective heat transfers from the transplant tray-substrate units to the inside air QC_{tr-a} at different growth stages is the summation of the convective heat from the transplant leaf and from the substrate soil surface to air, and is given by:

$$QC_{tr-a} = A_s \left[h_{s-a} + LAI \times h_{p-a}\right](T_{tr} - T_a) \quad (5)$$

where T_{tr} is the equivalent temperature of the tray-substrate unit, A_s is the substrate soil surface area (*i.e.*, the trays area), LAI is the leaf area index (leaves surface area/tray surface area) and h_{s-a}, h_{p-a} are the convective heat transfer coefficients between the substrate surface and air and between the transplant leaves and air, respectively. Correlation to estimate the convective coefficient, h_{p-a} is given by [32,33] as:

$$h_{p-a} = (k_a/L_p)\left[0.37Gr^{1/4}\right] \quad (6)$$

where Gr and L_p are the Grashof number and the leaf characteristic length (2 cm), respectively, and correlation to estimate h_{s-a} is given by [34] as:

$$h_{s-a} = Nu.k_a/L_s, \quad Nu = \begin{cases} 0.27Ra^{1/4}, & T_{tr} < T_a \\ 0.54Ra^{1/4} & T_{tr} > T_a \end{cases} \quad (7)$$

where L_s is the characteristic length of the substrate soil surface (*i.e.*, the tray length). The convective heat from the floor, uncovered with trays, Q_{f-a} in Equation (1) was estimated as $Q_{f-a} = A_f h_{f-a}(T_f - T_a)$. In the proposed closed solar house with FRC, h_{f-a} was assumed to be h_{s-a} (Equation (7)) and T_f equals to T_{tr}. Such assumptions did not jeopardize the accuracy of energy analysis in a closed solar house with FRC [30]. A_f was taken to be 0.35 of the total floor area of the house.

2.3. Transplant Tray-Substrate Unit

The transplants and the substrate (*i.e.*, soil matrix, water in the soil, transplant roots and air in the soil) are treated as one unit characterized by an average temperature T_{tr} and average thermo-physical properties. This is because the transplant's transpiration and the evaporation from the substrate were measured together as evapo-transpiration (ET) and the latent heat associated with the evapo-transpiration cannot be divided for plant and soil. The tray energy balance is given by:

$$QS_{\mathrm{tr}} + QT_{\mathrm{tr}} - QE_{tr} - QC_{\mathrm{tr-a}} - \kappa ET = \frac{d}{dt}\left[\rho V C_{\mathrm{p}} T\right]_{\mathrm{tr}} \quad (8)$$

The solar radiation absorbed by the trays at specified solar incidence (QS_{tr}) and the thermal radiation absorbed by the trays (QT_{tr}) are defined, respectively, by:

$$QS_{\mathrm{tr}} = A_c(1 - \rho_{\mathrm{se}})\overline{\tau}_{\mathrm{c}} G \quad (9)$$

$$QT_{\mathrm{tr}} = (1 - \rho_{\ell \mathrm{e}})\left\{QE_{\mathrm{c2}} + \rho_{\mathrm{c2}} QE_{\mathrm{tr}}\right\} \quad (10)$$

where ρ_{se} is the total effective short wave reflectance (albedo) of the trays at specified incident direction and $\rho_{\ell \mathrm{e}}$ is the total effective long wave reflectance of the tray. In addition, $\overline{\tau}_{\mathrm{c}}$ and G are the short wave cover transmittance and the solar radiation flux incident over the fluid-roof cover at the specified incident direction, respectively. The emissive power from the inner surface of the cover QE_{c2} is given by:

$$QE_{\mathrm{c2}} = N_c \sum_{i=1}^{N} A_i E_{\mathrm{c2,i}} \quad (11)$$

where N is the number of cover division in the channel and N_{c} is the number of channels in the cover. In fact, $E_{\mathrm{c2,i}}$ is a function of the spectral directional emissivity of the cover $\varepsilon_{\mathrm{c}}(\lambda, \theta)$ and the black body distribution function $I_{\mathrm{c}}(\lambda, T_{\mathrm{c2,i}})$. For simplicity, the emissive power from the cover element i ($E_{\mathrm{c2,i}}$), per unit area, was correlated as a function of the element temperature $T_{\mathrm{c2,i}}$ and reported in [30] as:

$$E_{\mathrm{c2,i}} = 1179.6 - 10614(T_{\mathrm{c2,i}}) + 0.027(T_{\mathrm{c2,i}})^2, \qquad \mathrm{R}^2 = 0.96 \quad (12)$$

The transplant tray was assumed as gray surface and the emission from the transplant trays QE_{tr} is defined as:

$$QE_{\mathrm{tr}} = A_{\mathrm{tr}} \varepsilon_{\mathrm{tr}} \sigma T_{\mathrm{tr}}^4 \quad (13)$$

The emittance of the transplant trays $\varepsilon_{\mathrm{tr}}$ was assumed to be constant value and equals to 0.90 and σ is the Stefan–Boltzmann constant [35,36].

2.4. Simulation Procedure

For the components of the fluid-roof cover system (Figure 2), the temperature profiles of the upper sheet (T_{c1}), lower sheet (T_{c2}), web (T_{w}) and LRF (T_{f}) were obtained by solving the 4-N differential equations describing the energy balance of these components; detailed analysis and method of solution were reported in [30]. The unknowns T_{a} and T_{tr} were obtained by solving Equations (1)–(8) simultaneously using Predictor Corrector Method [37]. The meteorological data used to solve these equations, such as the ambient temperature, wind speed and solar radiation flux, were recorded during 16 consecutive clear sunny days (the production period). In addition, required parameters used in the simulation, such as the leaf area index (LAI), transplant volume and density (V_{p}, ρ_{p}), tray evapo-transpiration (ET), water content in the substrate (W_{sub}) and physical and radiative properties of the transplant tray-substrate unit were measured in the conventional evaporation-cooled greenhouse and adapted to be useful in the proposed fluid-roof solar house. For example, the water content in the substrate soil, W_{sub}, measured in the greenhouse cannot be used directly as an input parameter for the simulation of the closed solar house because the environment is different; however, the ratio between W_{sub} and the cumulative evapo-transpiration can be used (more details are in Section 3.6).

3. Measuring and Estimating the Required Parameters

Experiments to determine the required parameters used in this study were conducted in the Agricultural Research and Experiment Station, Agriculture Engineering Department, King Saud University (Riyadh, Saudi Arabia, 46°47′ E, longitude and 24°39′ N, latitude). The proposed solar

house (32 m^2 floor area) dimensions, orientation (N–S) and the modes of energy exchanges through the house are illustrated in Figure 1a. An evaporation-cooled greenhouse with a floor area of 32 m^2 was used to grow the transplants. In the greenhouse and in the proposed solar house, the trays (Figure 1b) were arranged into three rows in the N–S direction (0.75 m width for each); the surface area covered with transplant trays was estimated to be 65% of the floor area. The remaining 35% of the floor area was a dry bare soil (four lanes) used for labor movement to serve the trays. Cabbage, (*Brassica campestris* L.) transplants were grown in the trays for 16 sunny days (the production period 1–16 May 2015) using artificial soil as supporting material. The measured meteorological parameters inside and outside the greenhouse were: (i) the air temperatures using aspirated psychrometers; (ii) the global solar radiation fluxes using CMP3 solar meters (Kipp & Zonen B.V. Inc., Bohemia, NY, USA); and (iii) the photosynthetically active radiation fluxes (PAR) using quantum sensors LI-190SA (LI-COR Inc., Lincoln, NE, USA). The other parameters used in the simulation modeling were estimated as follows.

3.1. Leaf Area Index (LAI)

Leaf area per transplant was measured at different growth stages during the production period (on Days 6, 9, 12 and 16 after sowing) using one tray. The *LAI* was estimated (leaf area per transplant × number of transplants per tray (*i.e.*, 128) divided by the tray area (*i.e.*, 0.18 m^2)) and plotted in Figure 3 at different days after sowing and could be correlated as a function of the day number after sowing (d) as follows:

$$LAI = 0.36 - 0.315(d) + 0.059(d)^2 - 0.002(d)^3, \qquad R^2 = 0.98 \tag{14}$$

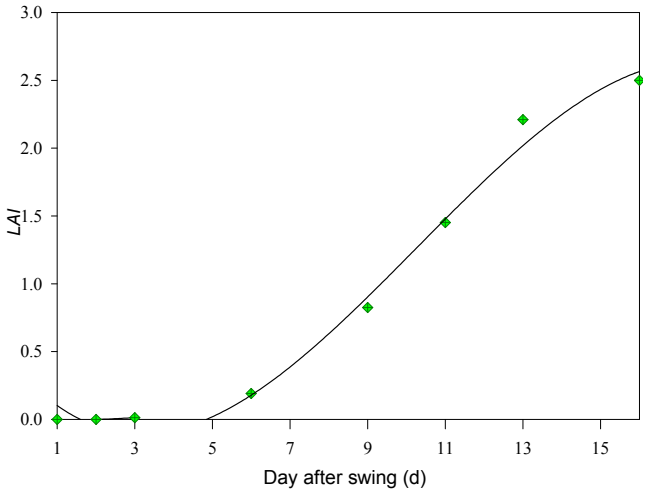

Figure 3. The measured (scattered points) and estimated (curve fitting) *LAI* on different days after sowing in the evaporatively-cooled greenhouse.

3.2. Transplants Volume (V_p)

The transplant volume, V_p was estimated at different growth stages by measuring the mass of fresh transplants (including the roots), m_p using electronic balance (EB-6200) and plotted in Figure 4. Average transplant density ρ_p was estimated to be equal to 720 kg·m^{-3} and m_p could be correlated as a function of d as follows:

$$m_p = 36.345 - 37.69(d) + 8.32(d)^2 - 0.16(d)^3, \qquad R^2 = 0.99 \tag{15}$$

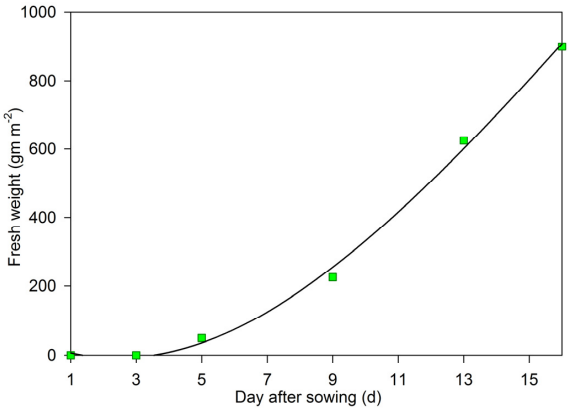

Figure 4. The measured (square points) and estimated (curve fitting) weight of the fresh transplants per unit area of tray on different days after sowing.

3.3. Evapo-Transpiration Rate (ET)

Tray weight was recorded every 5 min using an electronic balance (EB-6200) every day from Day 3 to Day 16 after sowing in the greenhouse. Thus, Evapo-transpiration rates *ET*, per unit area of tray, have been estimated. Hourly average values of *ET* have been plotted *vs.* the transmitted solar radiation flux into the greenhouse ($\overline{\tau}_c G$) every day during the production period. In CTPS, the daily average of *ET* was almost the same during the production period, except for the first three days (germination period) due to the steady state controlled environment in CTPS [8]. Similarly, in a closed solar house in sunny regions, the environment is expected to also be steady and the daily average of *ET* is expected to be nearly uniform during the production period. Therefore, correlations representing *ET* can be used for all the days in production period. Two correlations for the hourly average values of *ET* were obtained before noon and after noon (Figures 5 and 6) by fitting the values of ($\overline{\tau}_c G$) *vs. ET* for the production period. These correlations are given as follows:

(Before noon, 12:00 a.m.–12:00 p.m.)

$$ET = 1.024 + 0.322(\overline{\tau}_{sc} G) + 0.0001(\overline{\tau}_{sc} G)^2, \qquad R^2 = 0.86 \tag{16}$$

(After noon, 12:00 p.m.–12:00 a.m.)

$$ET = 20.59 + 0.43(\overline{\tau}_{sc} G) - 4.45 \times 10^{-4}(\overline{\tau}_{sc} G)^2, \qquad R^2 = 0.86 \tag{17}$$

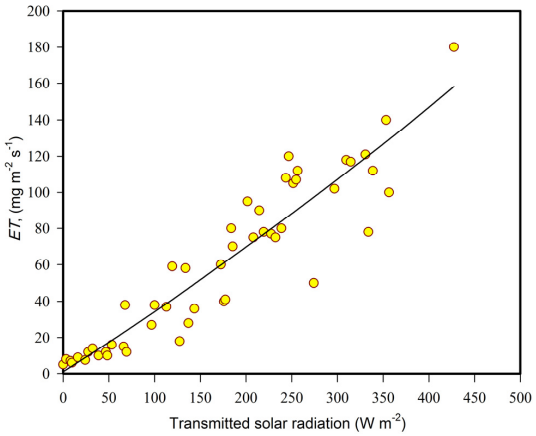

Figure 5. Evapo-transpiration rate before noon as a function of the transmitted solar radiation into the greenhouse.

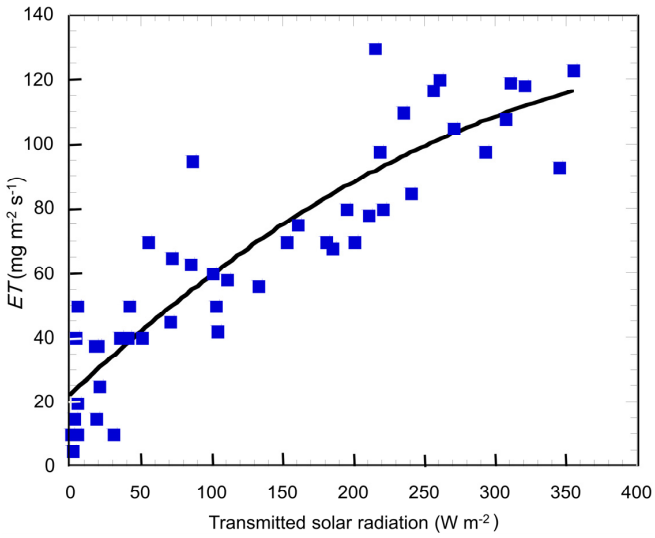

Figure 6. Evapo-transpiration rate after noon as a function of the transmitted solar radiation into the greenhouse.

3.4. Transplant Body and Soil Temperature (T_{tr})

The transplant trays including the soil substrate and the transplants were characterized by an average temperature, T_{tr}. To emphasize this assumption, the plant body temperature and the soil substrate temperature were measured on Day 10 (the substrate was fully covered with transplants) using a sheathed thermocouple (cupper constantan, T-type, 0.2 mm dia.) and recorded at 5 min intervals using a data logger (CR23X Micro-logger, Campbell Scientific, Inc., Logan, UT, USA). Figure 7 illustrates the plant body, the substrate, the greenhouse air and the outside ambient temperatures. As shown in Figure 7, the plant body and soil substrate temperatures are almost the same and the greenhouse air temperature during daytime is much higher than the outside ambient temperature in the naturally ventilated greenhouse used for measurements. However, the conventional ventilated (natural or forced) greenhouse cannot be used in hot and sunny regions for transplant production purposes due to the excessive solar radiation and extremely high air temperature.

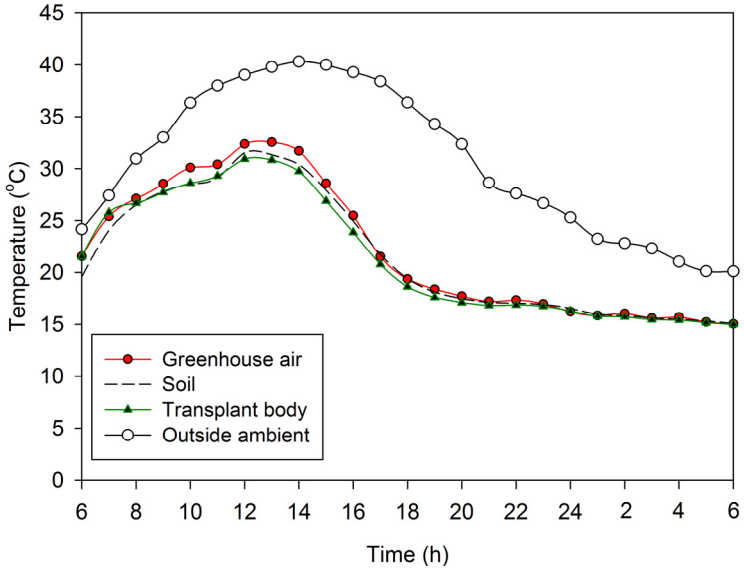

Figure 7. Time course of the transplant body, soil and air temperatures in the greenhouse compared with the outside ambient temperature.

3.5. Tray Radiative Properties

Trays short wave reflectance ρ_{se} (*i.e.*, apparent reflectance of transplant trays due to multiple reflections of solar beams between the transplant leaf and substrate) was recorded every 1 min, averaged every 30 min, and illustrated in Figure 8 for Day 1 and Day 15 (the beginning and end of the production period). Albedo-meter CMA-11 (Kipp & Zonen B.V. Inc., Bohemia, NY, USA) was used and the measured data were recorded in a data logger (CR23 Micrologger Campbell Scientific Inc., Logan, UT, USA). Value of ρ_{se} was taken from Figure 8 at each time interval at every day after sowing and used as input parameter in the simulation (for growing transplants in the proposed solar house). Long wave effective reflectance of the trays $\rho_{\ell\, e}$ was assumed to be constant value and equal to 0.1 [35].

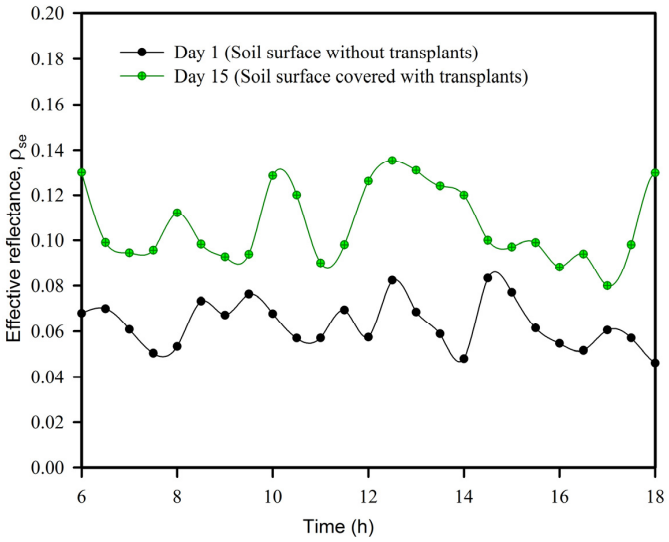

Figure 8. Time course of the effective reflectance of the transplant tray to solar radiation at the beginning and end of the production period.

3.6. Soil Matrix

Artificial soil was used in the study (*i.e.*, the substrate) consisting of 70% vermiculite, 20% peat and 10% sand by volume. Time courses of water content in the substrate (W_{sub}), dependent on *ET*, have been estimated during the production period in the greenhouse. Similar trends of W_{sub} were observed from Day 1 to Day 16 (sunny days). Therefore, Day 10 was chosen to represent time course of W_{sub} and the cumulative evapo-transpiration (*CET*) in the greenhouse (Figure 9). The W_{sub} time function (*i.e.*, decreasing of water content in the substrate) in the greenhouse cannot be used directly for the simulation in the proposed fluid-roof solar house. This is because the environmental conditions such as air temperature, relative humidity and solar radiation intensity affecting *ET* as well as W_{sub} in the greenhouse are different from those in the closed solar house. *ET* in Equation (1) is estimated in the solar house using Equations (16) and (17) based on the transmitted solar radiation into the house and the FRC transmittance; consequently, the *CET* can be estimated. To estimate the diurnal variation of W_{sub} inside the solar house, the ratio between W_{sub} and *CET* (Figure 10) was determined and W_{sub} was correlated in Equation (18) to be used in the solar house.

$$W_{sub} = CET \sum_{L=0}^{7} C_L(t)^L, \qquad R^2 = 0.95 \tag{18}$$

where t is the local time (in hour) and the coefficients C_L are: (C_o = 37,761, C_1 = −22,100, C_2 = 5468.4, C_3 = −741.14, C_4 = 59.426, C_5 = −2.8199, C_6 = 0.073359 and C_7 = 0.0008075).

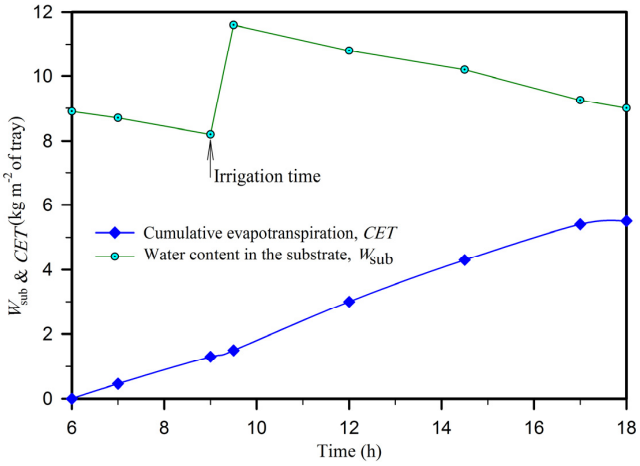

Figure 9. Time course of the water content in the substrate (W_{sub}) and the cumulative evapo-transpiration (CET) per unit area of trays.

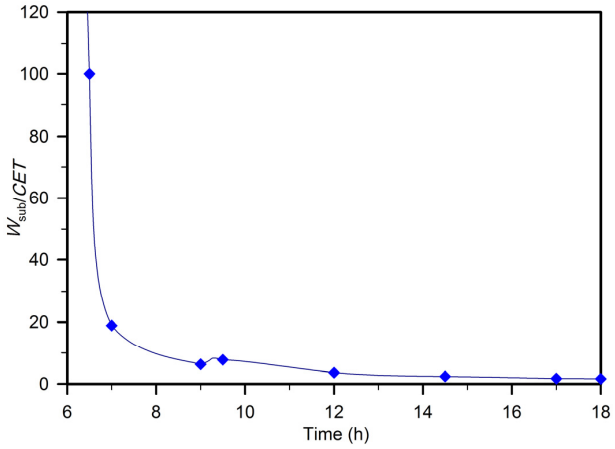

Figure 10. Time course of the ratio between water content in the substrate (W_{sub}) and cumulative evapo-transpiration (CET).

The decrease in W_{sub} with time was assumed to be replaced by air. Physical properties of soil compositions (vermiculite, peat and sand) were obtained from [35] and those for air and water were obtained from [36]. Accordingly, average thermo-physical properties of substrate are given by:

$$\rho_{sub} = \frac{\rho_v V_v + \rho_p V_p + \rho_s V_s + \rho_w V_w + \rho_a V_a}{V_{sub}} \quad (19)$$

$$Cp_{sub} = \frac{m_v Cp_v + m_p Cp_p + m_s Cp_s + m_w Cp_w + m_a Cp_a}{\rho_{sub} V_{sub}} \quad (20)$$

where the subscripts v, p, s, w and a are referring to substrate contents of vermiculite, peat, sand, water and air, respectively. Tray average properties including substrate and transplants (Cp_{tr} and ρ_{tr}) can be obtained by the same manner of Equations (19) and (20).

4. Results and Discussion

Time courses of the incident (measured) and the transmitted (estimated) photosynthetic photon flux (PPF) into the proposed fluid-roof solar house are illustrated in Figure 11 on two sunny summer days (May 1 and 15, 2015) for 12 h photo period (from 6:00 a.m. to 6:00 p.m.). Figure 11 shows that the transmitted PPF into the solar house is lower than 200 μmole· m^{-2}· s^{-1} (Wm^{-2} = 4.628 μmole· m^{-2}· s^{-1})

during short periods around sunrise and sunset and about 1200 μmole·m^{-2}·s^{-1} around noon. However, the optimum PPF for transplant production is generally 250–350 μmole·m^{-2}·s^{-1} [4,7]. This means that, during most of the day, the transmitted PPF is much higher than the transplant production demands. This leads to the possibility of using multi-shelves of transplant trays and radiation reflectors in the solar house to effectively distribute the excessive PPF to the trays. This in turn increases the house space utilization and increases the transplant production per unit area.

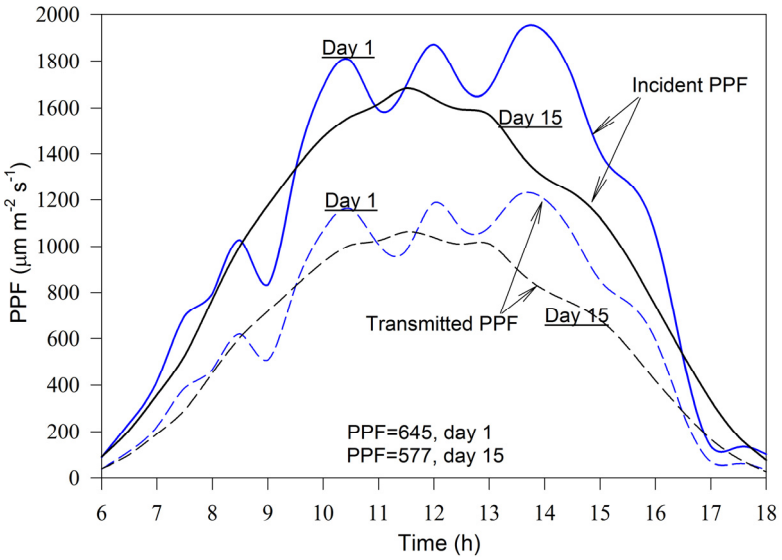

Figure 11. Diurnal incident (measured) and transmitted (simulated) photosynthetic photon flux (PPF) into the proposed solar house on sunny summer days (May 1 and 15, 2015) in Riyadh area.

Time courses of air temperature (T_a) inside the house and transplant tray temperature (T_{tr}) for two days (1 and 15 May 2015) during the production period compared with the outside ambient temperature (T_{am}) are illustrated in Figure 12a,b, showing that the fluid-roof solar house can reduce the inside air and transplant-tray temperatures (T_a, T_{tr}) by about 8–10 °C lower than the outside ambient temperature (T_{am}) through the production period in hot summer days. The energy released with evapo-transpiration reduces T_{tr} lower than T_a all the time. However, the value of T_a is higher than T_{tr} at earlier growth stages (Figure 12a, day 1) and is almost equal to T_{tr} at later growth stages (Figure 12b, day 15). This is due to the relatively low thermal energy absorbed by transplants at low growth stages and most of solar and thermal radiation inside the house is converted into convection heat transfer to the inside air via the house roof inner surface and transplant tray surfaces, which increases the internal energy of the air as well as its temperature T_a. The sidewalls and the FRC of the house act as thermal insulators, preventing the outside thermal energy to transmit into the house; therefore, such house can keep T_a and T_{tr} lower than T_{am}, even at nighttime.

Daily amount of the evapo-transpired water in the solar house estimated using Equations (16) and (17) compared with the measured values in the greenhouse and in the CTPS [8] are illustrated in Figure 13. Values of *ET* strongly depend on the relative humidity of the inside air and the vapor pressure deficit as well. Therefore, the integrated values of *ET* in the greenhouse fluctuate due to the variation of *RH* during the production period. Nearly uniform estimated values were obtained in the solar house due to the assumption of constant relative humidity (RH = 70%) during the production period. Values in the CTPS do not fluctuate much because of the steady state condition during the production period (which lasted for 11 days), except for values on first two days, which were lower due to the decrease of the controlled PPF in the germinating stage.

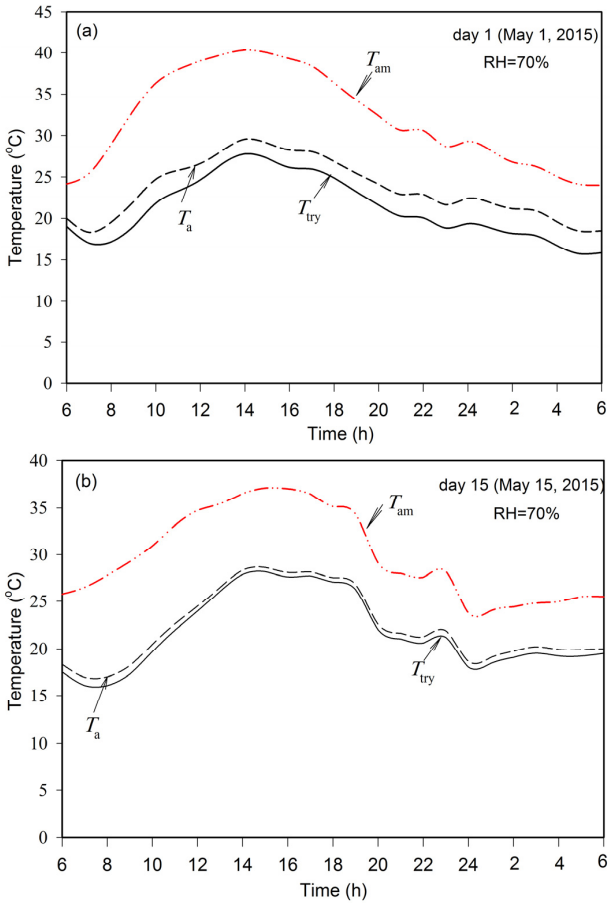

Figure 12. Time course of the simulated air and transplant tray temperatures inside the proposed solar house compared with the outside ambient temperature during 24-h: (**a**) day 1 and (**b**) day 15 of the production period.

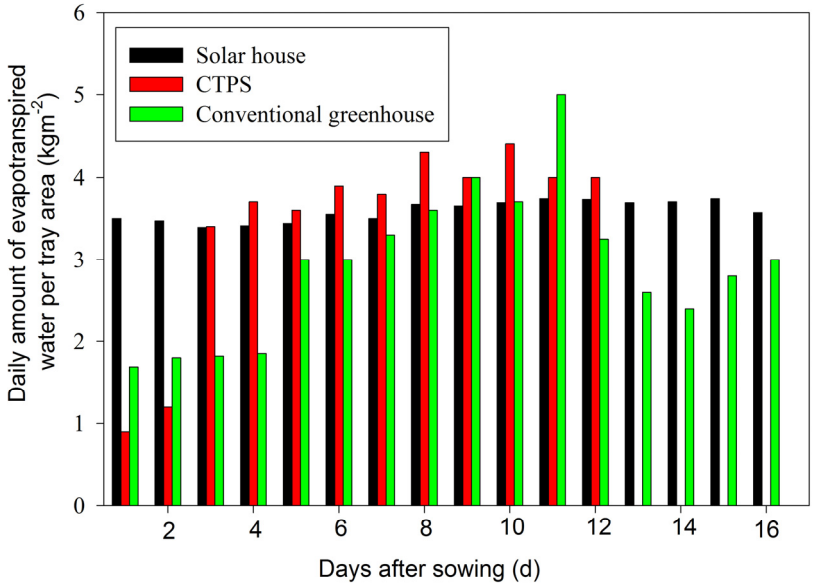

Figure 13. Comparison between daily amounts of evapo-transpired water measured in the CTPS and in the greenhouse and values obtained from the simulation of the solar house during the production period.

A schematic diagram of the daily integral of solar and thermal radiation energy distributed among the components of the solar house (MJ per unit area of tray) is illustrated in Figure 14. Sky thermal radiation together with some of solar radiation is absorbed completely in the cover system (about 14.1 MJ· m^{-2}· d^{-1}). Some of the absorbed energy was removed by the LRF and the rest is converted in the cover to internal energy. Around 70% of the transmitted PAR (10.8 MJ· m^{-2}· d^{-1}) is converted to latent heat during the evapo-transpiration process and 15% is converted to radiation emission and/or convection from the tray surface to the surrounding air inside the house. The remaining 15% of the transmitted PAR is reflected backward and assumed to escape from the cover to outside ambient because the cover has high PAR transmittance.

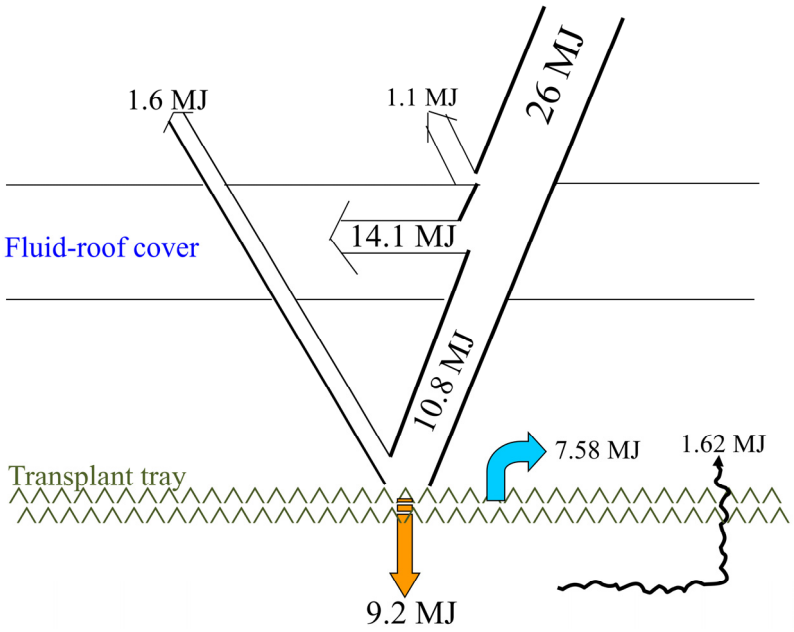

Figure 14. Schematic diagram of daily integral of solar and thermal energy flow distribution in the solar house per unit area of tray.

Electric energy consumption in the proposed solar house is mainly consumed for cooling the LRF, W_c (water cooler) and for dehumidifying the house air to maintain 70% *RH* in the house, W_d (dehumidifier). Minor electric energy consumption for auxiliaries' equipment, W_e, such as air circulating fans and LRF pumping was estimated to be around 3.2 MJ· m^{-2} during the production period. Electric energy consumption for air conditioning, W_a, (if T_a > 25 °C), water cooler and dehumidifier operate under hot condition were included as heat pump with a coefficient of performance (COP) equal to 2.5. Accordingly, cumulative power consumption, *i.e.*, W_c, W_a, W_d and W_e, during production period compared with CTPS electric energy consumption is illustrated in Figure 15. This figure shows that the energy consumption in the fluid-roof solar house is lower than that in CTPS because the energy for lighting (75% of the total energy consumption) is free in the solar house. Total electric energy consumption during the production period for the solar house was 183 MJ· m^{-2} (50.83 kWh· m^{-2}) while in CTPS it was 430 MJ· m^{-2} (119.4 kWh· m^{-2}). In sunny regions with extensive solar irradiance, the electric energy needed for the solar house can be supplied renewably using PV solar panels to supply the required electric energy to the house.

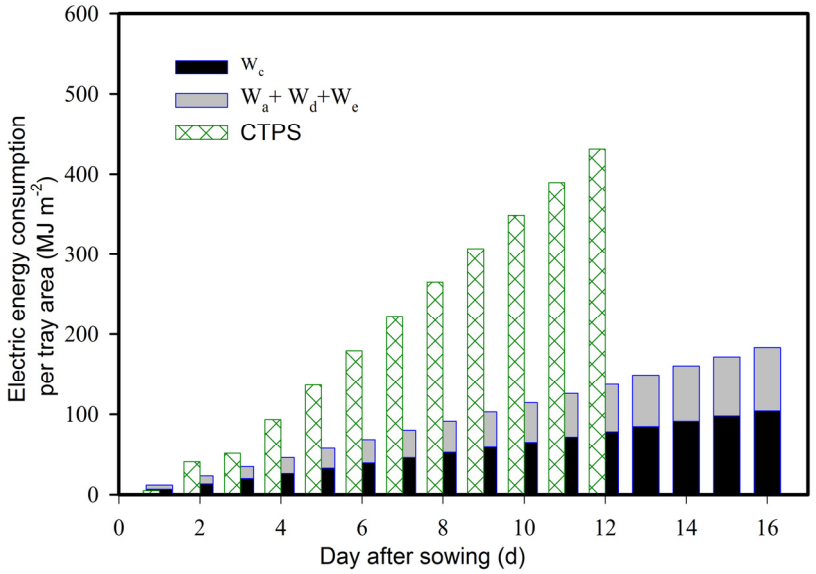

Figure 15. Accumulated daily integral of the total electric energy consumption in the solar house compared with the electric energy consumption in CTPS per unit area of tray.

5. Conclusions and Recommendations

According to the previous results and discussion, the conclusion can be summarized as follows:

1. Fluid-roof solar house can be used economically for transplant production in arid regions (usually hot sunny desert) where electric energy resources are not prevalent.
2. High values of PPF are transmitted into the house every day; thus, the house space could be better utilized using radiation reflectors and growing transplants in multi-layers of trays arranged in tray shelves.
3. The electric energy consumption in the proposed solar house was around 43% of the electric energy consumed in CTPS. This proves the profitability of using closed solar houses in arid regions.
4. Using $CuSO_4$-water solution as LRF may not be safe due to the possible leakage from the cover over the trays; however, at the moment, there is no alternative, cheap LRF available to use for absorbing the NIR effectively. Further research is needed to develop effective, safe and suitable LRFs for cooling the roofs of residential and agricultural structures.

Acknowledgments: The authors extend their sincere appreciation to the Deanship of Scientific Research at King Saud University for its funding of this research through the Research Group No. RG-1435-074.

Author Contributions: Abdel-Ghany was responsible for overall coordination of the research team and wrote the thermal analysis. Shady and Abdullah Ibrahim conducted the experiment and collected data. Al-Helal and Alsadon were involved in writing the manuscript and discussing the results. All the authors have read and approved the manuscript.

Conflicts of Interest: The authors declare no conflict of interest.

Nomenclature

A	area (m^2)
C_p	specific heat or volumetric heat capacity ($J \cdot kg^{-1} \cdot {}^\circ C^{-1}$ or $J \cdot m^{-3} \cdot {}^\circ C^{-1}$)
d	day number after sowing
ET	evapo-transpiration rate per unit area of floor ($mg \cdot m^{-2} \cdot s^{-1}$)
G	global incident solar radiation flux ($W \cdot m^{-2}$)
h	convective heat transfer coefficient ($W \cdot m^{-2} \cdot {}^\circ C^{-1}$)

I	black body radiation intensity ($W \cdot m^{-2} \cdot \mu m^{-1} \cdot sr^{-1}$)
LAI	leaf area index (-)
m	mass (kg)
N	number of cover divisions
Nc	number of channels in the cover
QC	convective energy rate (W)
QE	emissive power (W)
QS	absorbed solar radiation power (W)
QT	thermal radiation power (W)
t	time (s)
T	temperature (°C)
V	volume (m^3)
W	water content (kg)

Greek symbols

α	absorptance (-)
ε	emittance (-)
κ	latent heat of vaporization of water ($J \cdot kg^{-1}$)
λ	wave length (nm or μm)
θ	incident angle (degree)
ρ	reflectance (-) or density ($kg\ m^{-3}$)
$\overline{\tau}_c$	fluid-roof cover transmittance to solar radiation (-)

Subscripts

a	house air
am	ambient outside the house
c	cover
c1	upper sheet of the cover
c2	lower sheet of the cover
f	LRF or floor
I	cover element number
p	transplants
sub	substrate soil
tr	transplant tray
w	web

Abbreviations

CET	cumulative evapo-transpiration
CTPS	closed type production system
FRC	fluid-roof cover
LRF	liquid radiation filter
NIR	near infra-red radiation (700–2500 nm)
OTPS	open type production system
PAR	photosynthetically active radiation (400–700 nm)
PPF	photosynthetic photon flux (400–700 nm)

References

1. Kozai, T. Plant factory in Japan-current situation and perspectives. *Chron. Hortic.* **2013**, *53*, 8–11.
2. Jiang, H.-L.; Li, N.-J.; Xu, A.-D.; Yang, C.; Wang, H.-F.; Chen, H.-T.; Shan, P.-X.; Ding, W. Development of closed-type transplant production system and discussion of its application mode for flue-cured tobacco. *Aust. J. Crop Sci.* **2014**, *8*, 1566–1570.
3. Kozai, T.; Chun, C. Closed systems with artificial lighting for production of high quality transplants using minimum resource and environmental pollution. *Acta Hortic.* **2002**, *578*, 27–33. [CrossRef]
4. Yamada, C.; Ohyama, K.; Kozai, T. Photosynthetic photon flux control for reducing electric energy consumption in a closed-type transplant production system. *Environ. Control Biol.* **2000**, *38*, 255–261. [CrossRef]
5. Islam, A.F.M.S.; Chun, C.; Takagaki, M.; Sakami, K.; Kozai, T. Yield and growth of Sweet-potato using plug transplants as affected by their ages and planting depths. In *Transplant Production in the 21st Century*; Kluwer Academic Publisher: Dordrecht, The Netherlands, 2000; pp. 149–153.
6. Kozai, T.; Kubota, C.; Chun, C.; Afreen, F.; Ohyama, K. Necessity and concept of the closed transplant production system. In *Transplant Production in the 21st Century*; Kluwer Academic Publisher: Dordrecht, The Netherlands, 2000; pp. 3–19.
7. Kozai, T.; Ohyama, K.; Afreen, F.; Zobayed, S.; Kubota, C.; Hoshi, T.; Chun, C. Transplant production in closed systems with artificial lighting for solving global issues on environment conservation, food, resource and energy. In Proceedings of the ACESYS III Conference, Rutgers, NJ, USA, 23 July 1999; pp. 31–48.
8. Ohyama, K.; Fujiwara, M.; Kozai, T.; Kimura, H. Water consumption and utilization efficiency of a closed-type transplant production system. In Proceedings of the American Society of Agric. Engineers (ASAE) Annual Meeting, Milwaukee, WI, USA, 9–12 July 2000; pp. 1–8.
9. Kozai, T. Resource use efficiency of closed plant production system with artificial light: Concept, estimation and application to plant factory. *Proc. Jpn. Acad. Ser. B Phys. Biol. Sci.* **2013**, *89*, 447–461. [CrossRef] [PubMed]
10. Ohyama, K.; Oshinaga, Y.; Kozai, T. Energy and mass balance of a closed-type transplant production system: (part I)-Energy balance. *Jpn J. Soc. High Tech. Agric.* **2000**, *12*, 160–167. [CrossRef]
11. Al-Helal, I.M.; Abdel-Ghany, A.M. Energy partition and conversion of solar and thermal radiation into sensible and latent heat in a greenhouse under arid conditions. *Energy Build.* **2011**, *43*, 1740–1747. [CrossRef]
12. Kamel, M.A.; Shalaby, S.A.; Mostafa, S.S. Solar radiation over Egypt: Comparison of predicted and measured meteorological data. *Solar Energy* **1993**, *50*, 463–467. [CrossRef]
13. Van der Heyden, W. Sanitary House. *U.S. Patent*, 5 September 1893. Available online: http://patentimages.storage.googleapis.com/pdfs/US504544.pdf (accessed on 18 February 2016).
14. Van Bavel, C.H.M.; Damagnez, J.; Sadler, E.J. The fluid-roof solar greenhouse: Energy budget analysis by simulation. *Agric. For. Meteorol.* **1981**, *23*, 61–76. [CrossRef]
15. Van Bavel, C.H.M.; Damagnez, J. Cooling greenhouse crops in a Mediterranean summer climate. *Acta Hortic.* **1981**, *115*, 527–536. [CrossRef]
16. Sadler, E.J.; van Bavel, C.H.M. Simulation and measurements of energy partition in a fluid-roof greenhouse. *Agric. For. Meteorol.* **1984**, *23*, 1–13. [CrossRef]
17. Kopel, R.; Gale, J.; Zeroni, M.; Levi, S. A greenhouse with selective radiation filtering roof under desert conditions. In Proceedings of the International Symposium on Applied Technology of Greenhouse, Beijing, China, 7–10 October 1991.
18. Zeroni, M.; Gale, J.; Kopel, R.; Levi, S. Agrotechniques for a closed greenhouse with a radiation filtering roof. In Proceedings of the International Symposium on Applied Technology of Greenhouse, Beijing, China, 7–10 October 1991.
19. McMahon, M.J.; Kelly, J.W.; Decoteau, D.R. Growth of dendranthema x grandiflorum (ramat.) kitamura under various spectral filters. *J. Am. Soc. Hort. Sci.* **1991**, *116*, 950–954.
20. Rajapakse, N.C.; Kelly, J.W. Regulation of chrysanthemum growth by spectral filters. *J. Amer. Soc. Hort. Sci.* **1992**, *117*, 481–485.
21. Rajapakse, N.C.; McMahon, M.J.; Kelly, J.W. End of day far-red light reverses height reduction of Chrysanthemum induced by $CuSO_4$ spectral filters. *Sci. Hort.* **1993**, *53*, 249–259. [CrossRef]
22. Rajapakse, N.C.; Kelly, J.W. Spectral filters and growing season influence growth and carbohydrate status of Chrysanthemum. *J. Am. Soc. Hort. Sci.* **1995**, *120*, 78–83.

23. Rajapakse, N.C.; Kelly, J.W. Spectral filters influence transpirational water loss in Chrysanthemum. *J. Am. Soc. Hort. Sci.* **1993**, *28*, 999–1001.
24. Levi, S.; Zeroni, M.; Gale, J.; Kopel, R. Development of liquid radiation filters for use in greenhouses. In Proceedings of the International Symposium on Applied Technology of Greenhouse, Beijing, China, 7–10 October 1991.
25. Feuermann, D.; Kopel, R.; Zeroni, M.; Levi, S.; Gale, J. Theory and validation of a liquid radiation filter greenhouse simulation for performance prediction. *Trans. ASAE* **1997**, *40*, 175–184. [CrossRef]
26. Feuermann, D.; Kopel, R.; Zeroni, M.; Levi, S.; Gale, J. Evaluation of a liquid radiation filter greenhouse in a desert environment. *Trans. ASAE* **1998**, *41*, 1781–1788. [CrossRef]
27. Syed, K.H.G.; Abdel-Ghany, A.M.; Al-Helal, I.M.; El-zahrani, S.M.; Alsadon, A.A. Evaluation of PE film having NIR-reflective additives for greenhouse applications. *Adv. Mater. Sci. Eng.* **2013**, *2013*, 575081. [CrossRef]
28. Abdel-Ghany, A.M.; Kozai, T.; Chun, C. Evaluation of selected greenhouse covers for use in regions with a hot climate. *Jpn. J. Trop. Agric.* **2001**, *45*, 242–250.
29. Abdel-Ghany, A.M.; Abdel-Shafi, N.Y.; Taha, I.S.; Huzayyin, A.S. Solar radiation transmission through a hollow-channelled fluid-roof greenhouse cover. *Bull. Fac. Eng. Assiut Univ. Egypt* **2000**, *28*, 55–72.
30. Abdel-Ghany, A.M.; Kozai, T.; Abdel- Shafi, N.Y.; Taha, I.S.; Huzayyin, A.S. Dynamic simulation modelling of heat and water vapour transfer in the fluid roof greenhouse. *Jpn. J. Agric. Meteorol.* **2001**, *57*, 169–182. [CrossRef]
31. Duffie, J.A.; Beckman, W.A. *Solar Engineering of Thermal Processes*, 2nd ed.; John Wiley & Sons Inc.: New York, NY, USA, 1991.
32. Stanghellini, C. Transpiration of Greenhouse Crops: An Aid to Climate Management. Ph.D. Thesis, Agricultural University, Wageningen, The Netherlands, 1987.
33. Stanghellini, C. Mixed convection above greenhouse crop canopies. *Agric. For. Meteorol.* **1993**, *66*, 111–117. [CrossRef]
34. Yang, X. Greenhouse Microclimate: Transport Process, Plant Responses and Dynamic Modeling. Ph.D. Thesis, The Ohio State University, Columbus, OH, USA, 1988.
35. Jury, W.A.; Gardner, W.R.; Gardner, W.H. *Soil Physics*, 5th ed.; John Wiley& Sons Inc.: Washington, DC, USA, 1991.
36. Holman, J.P. *Heat Transfer*, 8th ed.; McGraw-Hill, Inc.: New York, NY, USA, 1997.
37. Jacques, I.; Judd, C. *Numerical Analysis*; Chapman and Hall Inc.: London, UK, 1987.